https://doi.org/10.1016/j.msea.2016.05.090

Effect of external disturbances on the strain-rate dependent plastic deformation behavior of a bulk metallic glass

S.H. Chen*, T.M. Yue, C.P. Tsui and K.C. Chan

Advanced Manufacturing Technology Research Centre

Department of Industrial and Systems Engineering

The Hong Kong Polytechnic University

Hung Hom, Kowloon

Hong Kong

* Corresponding author. E-mail: s-h.chen@polyu.edu.hk, cshunhua@gmail.com

Abstract

In this work, the effect of external disturbances on the strain-rate dependent plastic deformation behavior of a $Zr_{57}Cu_{20}Al_{10}Ni_8Ti_5$ bulk metallic glass (BMG) has been examined by tailoring the geometric confinement, stress gradient, and sample size. With the external disturbances, the fracture strains of the BMG specimens become less dependence on the strain rates, and it is found that the confinement of the propagation of shear bands is the dominant deformation mechanism. This is different from previous findings in that multiplication of the shear bands also plays a critical role in accommodating the plastic deformation of BMGs with external disturbances. The present findings not only shed more light on the deformation mechanisms of BMGs under external disturbances, but also suggest that the use of external disturbances can reduce the dependence of the plastic deformation behavior of BMGs on the strain rates.

Key words: Bulk metallic glass; Plastic deformation; Geometric confinement; Stress gradient; Shear bands.

1. Introduction

During past decades, bulk metallic glasses (BMGs), as a new class of structural materials, have attracted great research interest due to their unique properties stemming from non-ordered atomic arrangements, such as superior mechanical properties compared with their crystalline counterparts [1-3]. Without crystalline lattices and defects, the plastic deformation in BMGs is characterized by intermittent bursts of shear events, demonstrating serrations in the stress-strain curves [4-6]. Many studies have shown that the deformation behavior of BMGs is significantly dependent on the strain rate [4,7-11], for example, the fracture behavior [7,12,13] and bursts of shear events [4,14]. With increasing strain rate, the plastic flow in BMGs tends to transit from serrated flow to non-serrated flow [4,14], and the critical strain rate is dependent on the physical nature of the alloys, such as the alloy composition [4,15]. The plastic-flow dynamics of BMGs can also be tuned by the change of strain rates [10]. Simulations of the plastic deformation of metallic glasses show that the yield stress [16-18] and shear transformation zone (STZ) characteristics [19,20] are also dependent on the applied strain rates. For example, Cao et al. [18] have reported the decrease of yield stress at relatively lower strain rates. Understanding the dependence of the plastic deformation behavior of BMGs on the change of strain rates is important before enabling wide applications as structural materials. Recently, Bhattacharyya et al. [11] examined the effect of the internal free volume content on the strain-rate sensitivity of the plastic flow in BMGs, and found that a higher free volume content can reduce the strain-rate sensitivity. However, previous findings have shown that the plastic deformation behavior of BMGs is affected by not only the internal physical properties of the BMGs, such as free volume [21], alloy composition [22-24] and Poisson's ratio [25,26], but also the applied external disturbances, such as geometric confinement [27-29], stress gradient [30-32] and sample size [33,34]. Under external disturbances, such as geometric confinement and the presence of stress gradients, BMGs are able to demonstrate more plastic deformation behavior, resulting from the multiplication of the shear bands and the confinement of their propagations [27,28,30,32,35]. However, how the strain-rate dependent plastic deformation

behavior is influenced by the external disturbances has not been documented. In this work, the effect of external disturbances on the strain-rate dependence of the plastic deformation behavior of a BMG is further examined and its deformation mechanism analyzed under different strain rates.

2. Experimental

2.1 Specimen preparation

As-cast $Zr_{57}Cu_{20}Al_{10}Ni_8Ti_5$ (at.%) BMG specimens were fabricated from the pure elements of Zr (99.8%), Cu (99.999%), Al (99.99%), Ni (99.999%) and Ti (99.995%). Master alloy ingots were firstly produced by arc-melting the pure elements using a WK-II vacuum arc melter under an Ar atmosphere. After remelting the master alloy ingots five times, cylindrical specimens of 3 mm and 2 mm diameters were fabricated by suction casting the melted alloy into water-cooled copper molds [32]. The amorphous nature of the as-cast rods was checked using X-ray diffraction (XRD) analysis on a Rigaku SmartLab X-ray diffractometer. To examine the effect of external disturbances on the strain-rate dependent plastic deformation behavior of BMGs, three kinds of external disturbances were introduced in this work: geometric confinement, stress gradient and sample sizes. Four groups of BMG specimens, with aspect ratios of 2, were produced from the cylindrical rods. As shown in the schematic diagram in Fig. 1, Group A and Group C specimens were cut from the cylindrical rods with 2 mm and 3 mm in diameters, respectively. After electro-depositing a Ni layer onto the 2 mm diameter cylindrical rods using an electrolyte and methods described in Ref. [27], Group B specimens with geometric confinement were cut from the coated rods. The Ni thicknesses of Group B specimens were 66 ± 7 μm. In Group D, a tilt angle of 2° was tailored on the top surface of the 3 mm diameter specimens, resulting in the presence of stress gradients under subsequent compression tests [30]. The morphology of the prepared specimens was inspected using optical microscopy (OM), and the results are shown in Fig. 1.

2.2 Compression tests

Compression tests were conducted on an MTS Qtest/25 materials testing machine at room temperature. The four groups of specimens were tested at strain rates of 5×10^{-3}, 5×10^{-4} and 5×10^{-5} s^{-1} respectively, and collected at a rate of 50 data per second. Three specimens for each condition were tested. After compressive testing, the specimens were inspected using scanning electron microscopy (SEM) on a JEOL JSM-6490 scanning electron microscope.

2.3 Finite Element Modelling (FEM) analysis

To characterize the yielding and the evolution of the yielded regions in the Group D specimens, the gradient stress distributions were simulated using FEM analysis based on a commercial ABAQUS package with an ideal elastic-plastic constitutive model [36,37]. Although such constitutive model cannot be used to simulate the nucleation and propagation of shear bands as well as the fracture of BMGs, it is good to characterize the evolution of yielded regions where shear bands are formed [36,37]. The input material parameters for the FEM analysis are 1.635 GPa for the yield stress [36], 82 GPa for Young's modulus [38] and 0.36 for Poisson's ratio [38].

3. Results

3.1 Effect of external disturbances on the nominal plasticity

The nominal stress-strain curves of four groups of specimens under different strain rates are given in Fig. 2. In Group A, the nominal strain increases significantly as the strain rate decreases (Fig. 2a,e), agreeing well with previous findings [7]. However, when external disturbances were applied to Groups C-D, this trend changed. For the Ni-coated specimens in Group B, they all demonstrated large nominal strains, reaching about 12%. It seems that the nominal plasticity of this group of specimens was not affected by the applied strain rates. As compared with the specimens in Group A without Ni coatings, Group B specimens show an enhanced nominal strain of 12.5% at a strain rate of 5×10^{-3} s^{-1}. At a strain rate of 5×10^{-5} s^{-1}, the nominal strains show no significant enhancement, and the decrease of strain rate tends to reduce the differences in the nominal strains between Groups A and B (Fig. 2b,e). With the increased sample

sizes in Group C, the nominal strains (2.4% - 4.3%) are smaller than the values in Group A, especially at the low strain rates. This suggests that the enhancement of the plasticity of the BMGs by reducing the strain rates is very limited at relatively large sample sizes (Fig. 2c,f). With the presence of stress gradients in Group D, the nominal strains are larger than the values in Group C, and the nominal strain also increases with the decrease of applied strain rate (Fig. 2d,f). However, the increasing rate is smaller as compared with Group A.

In order to quantify the dependence of the nominal strains on the change of strain rate, a scaling parameter, V, describing the variance of the nominal strains on the changing strain rates is proposed as

$$V = (\varepsilon_{-4} - \varepsilon_{-3})^2 + (\varepsilon_{-5} - \varepsilon_{-4})^2 \quad (1)$$

where ε_{-3}, ε_{-4} and ε_{-5} denote the average nominal strains at strain rates of 5×10^{-3}, 5×10^{-4} and 5×10^{-5} s^{-1}, respectively. The parameters V_A, V_B, V_C and V_D are calculated as 20.6, 4.3, 0.4, 14.8, respectively. It is clear that the specimens in Groups B-D with external disturbances have less variations in the nominal strains, i.e., less dependence on the applied strain rate, especially for Group B, with geometric confinement and Group C, with increased sample sizes.

3.2 Effect of external disturbances on the bursts of stress drops.

The plastic flow in the BMGs consists of intermittent bursts of shear events, which are correlated to the stress drops in the stress-strain curves [5]. With decreasing strain rates, the plastic flow transits from non-serrated flow to serrated flow at a critical strain rate [4,15]. It is obvious that the applied strain rates in the present work are higher than the critical strain rate of the BMG and serrated stress drops were observed in all specimens, as can be seen in Fig. 1 (Hu. et al. [14] reported a critical strain rate of about 5×10^{-2} s^{-1} in a Vit105 BMG with a similar composition of $Zr_{52.5}Ti_5Cu_{17.9}Ni_{14.6}Al_{10}$). To compare the burst of stress drops in the specimens with different nominal strains, the number of stress drops per 1% nominal strain (N/ε_n) of four groups of specimens was plotted in Fig. 3. It can be seen that the burst of stress

drops is significantly affected by the applied external disturbances. As compared with Group A, the geometric confined specimens in Group B have more stress drops at relatively higher strain rates (5×10^{-3} and 5×10^{-4} s^{-1}). For the Group C specimens with increased sample sizes, they have a larger number of stress drops at low strain rates (5×10^{-4} and 5×10^{-5} s^{-1}) than the Group A specimens. With the presence of stress gradients in Group D, the specimens have more stress drops in plastic flow than Group C specimens, especially at low strain rates (5×10^{-4} and 5×10^{-5} s^{-1}).

More shear events in BMGs (more stress drops on the stress-strain curves) are usually correlated to the BMG specimens with larger plasticity [39,40]. However, some different results are observed in the present study. As shown in Fig. 4, in Groups A and C, the number of stress drops are proportional to the fracture strains (indicated by the dash lines), and the linear relationship is independent on the sample size. Nonetheless, with the larger sample size in Group C, a higher increasing rate (a larger slope) was observed in Fig. 4. This suggests that to achieve same strains, more shear events must occur in the specimens with larger sample sizes. With the presence of geometric confinement (Group B) and stress gradient (Group D), the linear relationships have been changed. In Group B, although the number of stress drops changes at different strain rates, the nominal plasticity does not change significantly, i.e., even at a high strain rate of 5×10^{-3} s^{-1} with less stress drops, the specimens still display large nominal plasticity. In Group D, although the increase of fracture strains was still observed in the specimens with more stress drops, it does not follow a linear relationship like Groups A and C.

4. Discussion

4.1 Effect of geometric confinement

The plastic deformation of BMGs is accommodated by the activation and propagation of shear bands, which are affected by not only the intrinsic physical properties but also the extrinsic disturbances, such as complex stress fields [17]. Thus, the changes in the deformation mechanisms of BMGs under external disturbances may also induce

some differences in the strain-rate dependent plastic flow behavior. With geometric confinement, the mechanisms for the enhancement of the plastic deformation behavior are known to be twofold: to trigger the burst of multiple shear bands and to confine the propagation of the shear bands [27-29,41]. However, the present findings suggest that the confinement of the propagation of the shear bands plays a more significant role in improving the plastic deformation behavior of BMGs. On the one hand, although previous findings show more shear events in the BMG specimens with larger nominal plasticity, our statistical analysis results show that the number of shear events and the nominal plasticity do not follow a linear relationship in the geometric confined specimens (Fig. 4). At a high strain rate of 5×10^{-3} s^{-1}, although fewer shear events were observed, the specimen still manifested large nominal strains. Differing from the findings where the increase of shear events can result in the enhancement of plasticity in Group A, similar increases in the shear events at the relatively lower strain rates of 5×10^{-4} and 5×10^{-5} s^{-1} (Fig. 3) does not result in the improvement in the nominal strains, but a slight decrease (Fig. 2e). In other words, for the geometric confined BMG specimens, the nominal plasticity was not dependent on the multiplication of shear events. On the other hand, the burst of stress drops in the plastic flow of BMGs can be fitted using power law decay dynamics [39,40,42,43]. Based on the Levenberg-Marquardt algorithm, the cumulative distributions of the stress drops in the plastic flow were fitted using the equation [44]

$$P(P > \sigma_n) = \sigma_n^{-\beta} \exp(-\sigma_n/\sigma_c) \quad (2)$$

where σ_n is the stress drop, β is a scaling parameter and σ_c is the cut-off stress drop. With the exponent of β = 0.15, the cut-off stress drops of Groups A, B and D were given in Table I (Due to the small plasticity, only a few stress drops were collected in Group C, and the plastic-flow dynamics in this group were therefore not fitted using the power-law decay function). The relatively smaller cut-off stress drops in Group B specimens, especially at a high strain rate, indicate the decreased amplitude of the shear events and a stronger barrier to their propagation [44]. The impediment of the shearing process in the geometric confined BMGs was evidenced in the SEM images in Fig. 5. It can be seen that the shearing process has been stopped by the Ni-coating,

where corrugated Ni coatings were observed. Additionally, significant decrease of nominal stresses before failure in Group B (Fig. 2b) also implies that the fracture process has been significantly inhibited. Therefore, with geometric confinement, the enhancement of the plasticity is mainly controlled by the confinement of the propagation of the shear bands, rather than the burst of multiple shear bands.

4.2 Effect of stress gradient

In Group D specimens with stress gradients, the initiation and propagation of the shear bands are significantly affected by the evolution of the stress-concentrated regions, which are different from the deformation mechanisms under the relatively uniform stress states in Groups A and C. The gradient stress distributions in a Group D specimen with a nominal strain of 2.25% are shown in Fig. 6. The stress gradient can profuse the shear-band formation at the stress-concentrated regions and, at the same time, confine the propagation of the shear bands by the unyielded regions [32,45]. In the present work, the Group D specimens demonstrate different deformation behavior under varying strain rates. At a high strain rate of 5×10^{-3} s^{-1}, the number of shear events is slightly more than that of the Group C specimens, but the specimens demonstrate greatly enhanced nominal plasticity (Fig. 4). While at a relatively lower strain rate (5×10^{-4} s^{-1}), the specimens tend to burst more shear events. However, the increase in the nominal plasticity is small. This implies that the enhanced nominal plasticity at high strain rates (5×10^{-3} and 5×10^{-4} s^{-1}), as compared with the Group C specimens, can be mainly attributed to the confinement of the propagation of the existing shear bands by the unyielded regions. The confinement of the shear band propagation can be further evidenced by the small cut-off stress drops (σ_c = 13.8 MPa and 14.9 MPa, respectively) at high strain rates (5×10^{-3} and 5×10^{-4} s^{-1}), as shown in Table I. At a low strain rate of 5×10^{-5} s^{-1}, the enhancement in the nominal plasticity as compared with the specimens at a strain rate of 5×10^{-4} s^{-1} may be partially caused by the burst of multiple shear events (Fig. 4). The formation of multiple shear bands at the stress-concentrated regions is observed in the SEM images of a fractured specimen with a nominal strain of 13.6% (Fig. 7a,b). On the other hand,

the smallest cut-off stress drop (σ_c = 6.9 MPa) suggests that the confinement effect on the propagation of the shear bands is still very strong. The confinement effect can also be validated by the deflection of the fracture plane (Fig. 7a), where the fracture path has been impeded by a large number of curved shear bands (Fig. 7c). It is speculated that, at a low strain rate of 5×10^{-5} s^{-1}, both the multiplication of the shear bands and the confinement of their propagations play significant roles.

4.3 The dominant mechanisms under external disturbances

The dominant deformation mechanisms of the plastic deformation behavior of BMGs under external disturbances are summarized in Table II. The reduced strain-rate dependence of the plastic deformation behavior of BMGs was mainly controlled by the dominant mechanism of the confinement of the propagation of the shear bands. In the specimens where the confinement of the shear band propagation plays the dominant role, the nominal plasticity show less dependence on the change of strain rates, such as Group B specimens, and Group D specimens at relatively-high strain rates (from 5×10^{-3} to 5×10^{-4} s^{-1}). While in the specimens where the multiplication of the shear bands plays a significant role, the nominal plasticity show strong dependence on the applied strain rates, such as Group A and Group D at relatively-low strain rates (from 5×10^{-4} to 5×10^{-5} s^{-1}). It should be mentioned that in Group C specimens with increased sample sizes, the small variation in the nominal strains was due to the fact that all the specimens demonstrated limited nominal strains, ranging from 2.43% to 4.32%. Despite the small nominal plasticity, the number of shear events and the nominal plasticity still follows a linear relationship (Fig. 4), i.e., the plastic deformation behavior is still dependent on the applied strain rates, similar to Group A specimens. The burst of more shear bands in Group C specimens than Group A specimens may result from the large sample sizes where more casting defects exist and provide more sources for originating shear events [46]. The present work suggests that, in the practical applications of BMGs as structural materials, the use of external disturbances can reduce the dependence of the plastic deformation behavior on the change of strain rates. The present research is in line with the

previous findings of loading-rate-independent plastic flow in BMGs under a complex stress field [47], and provides more explanations for such a phenomenon where the confinement of the propagation of the shear bands also plays a significant role. Additionally, the findings provide some suggestions to improve the plastic deformation behavior of BMGs in practical applications, where the material always deforms under complex stress states and has a wide range of product dimensions and macroscopic structures [48-50]. For example, to improve the plastic deformation behavior of BMGs with large product dimensions, more attention might be paid to the confinement of the propagation of the shear bands using external disturbances, such as tailoring stress gradients in Group C specimens.

5. Conclusions

The effect of external disturbances on the plastic deformation behavior of BMGs at varying strain rates has been examined by tailoring the geometric confinement, stress gradient and sample size. The deformation mechanisms of BMGs under external disturbances have also been discussed. The findings show that for those specimens where the confinement of the propagation of shear bands plays a dominant role, the fracture strain is less sensitive to the applied strain rate. Whereas for the specimens where the multiplication of the shear bands plays a significant role, the fracture strain shows strong dependence on the applied strain rate. The findings give more insight into the deformation mechanisms of BMGs under external disturbances. It also suggests that, in practical applications, stable plastic deformation behavior of BMGs with the change of loading rates could be achieved by applying appropriate external disturbances.

Acknowledgements

The work described in this paper was fully supported by a grant from the Research Committee of the Hong Kong Polytechnic University under research project No. 1-YW0R.

References

[1] J. Plummer, W.L. Johnson, Is metallic glass poised to come of age?, Nat. Mater., 14 (2015) 553-555.

[2] M.M. Trexler, N.N. Thadhani, Mechanical properties of bulk metallic glasses, Prog. Mater. Sci., 55 (2010) 759-839.

[3] S.H. Chen, K.C. Chan, F.F. Wu, L. Xia, Achieving high energy absorption capacity in cellular bulk metallic glasses, Sci. Rep., 5 (2015) 10302.

[4] C.A. Schuh, T.G. Nieh, A nanoindentation study of serrated flow in bulk metallic glasses, Acta Mater., 51 (2003) 87-99.

[5] S.X. Song, H. Bei, J. Wadsworth, T.G. Nieh, Flow serration in a Zr-based bulk metallic glass in compression at low strain rates, Intermetallics, 16 (2008) 813-818.

[6] H.M. Chen, J.C. Huang, S.X. Song, T.G. Nieh, J.S.C. Jang, Flow serration and shear-band propagation in bulk metallic glasses, Appl. Phys. Lett., 94 (2009) 141914.

[7] T. Mukai, T.G. Nieh, Y. Kawamura, A. Inoue, K. Higashi, Effect of strain rate on compressive behavior of a Pd40Ni40P20 bulk metallic glass, Intermetallics, 10 (2002) 1071-1077.

[8] H. Bei, S. Xie, E.P. George, Softening caused by profuse shear banding in a bulk metallic glass, Phys. Rev. Lett., 96 (2006) 105503.

[9] J.L. Ren, C. Chen, G. Wang, N. Mattern, J. Eckert, Dynamics of serrated flow in a bulk metallic glass, AIP Adv., 1 (2011) 032158.

[10] J. Antonaglia, X. Xie, G. Schwarz, M. Wraith, J.W. Qiao, Y. Zhang, P.K. Liaw, J.T. Uhl, K.A. Dahmen, Tuned Critical Avalanche Scaling in Bulk Metallic Glasses, Sci. Rep., 4 (2014) 4382.

[11] A. Bhattacharyya, G. Singh, K.E. Prasad, R. Narasimhan, U. Ramamurty, On the strain rate sensitivity of plastic flow in metallic glasses, Mater. Sci. Eng. A, 625 (2015) 245-251.

[12] T.C. Hufnagel, T. Jiao, Y. Li, L.Q. Xing, K.T. Ramesh, Deformation and failure of Zr57Ti5CU20Ni8Al10 bulk metallic glass under quasi-static and dynamic compression, J. Mater. Res., 17 (2002) 1441-1445.

[13] L.H. Dai, L.F. Liu, Y.L. Bai, B.C. Wei, G.S. Yu, Strain rate-dependent

compressive deformation behavior of Nd-based bulk metallic glass, Intermetallics, 13 (2005) 827-832.

[14] J. Hu, B.A. Sun, Y. Yang, C.T. Liu, S. Pauly, Y.X. Weng, J. Eckert, Intrinsic versus extrinsic effects on serrated flow of bulk metallic glasses, Intermetallics, 66 (2015) 31-39.

[15] C.A. Schuh, A.S. Argon, T.G. Nieh, J. Wadsworth, The transition from localized to homogeneous plasticity during nanoindentation of an amorphous metal, Philos. Mag., 83 (2003) 2585-2597.

[16] Y.Q. Cheng, E. Ma, Intrinsic shear strength of metallic glass, Acta Mater., 59 (2011) 1800-1807.

[17] A.L. Greer, Y.Q. Cheng, E. Ma, Shear bands in metallic glasses, Mater. Sci. Eng. R, 74 (2013) 71-132.

[18] P.H. Cao, X. Lin, H.S. Park, Strain-rate and temperature dependence of yield stress of amorphous solids via a self-learning metabasin escape algorithm, J. Mech. Phys. Solids, 68 (2014) 239-250.

[19] P.H. Cao, H.S. Park, X. Lin, Strain-rate and temperature-driven transition in the shear transformation zone for two-dimensional amorphous solids, Phys. Rev. E, 88 (2013) 042404.

[20] P.H. Cao, X. Lin, H.S. Park, Surface shear-transformation zones in amorphous solids, Phys. Rev. E, 90 (2014) 012311.

[21] L.Y. Chen, A.D. Setyawan, H. Kato, A. Inoue, G.Q. Zhang, J. Saida, X.D. Wang, Q.P. Cao, J.Z. Jiang, Free-volume-induced enhancement of plasticity in a monolithic bulk metallic glass at room temperature, Scripta Mater., 59 (2008) 75-78.

[22] Y.H. Liu, G. Wang, R.J. Wang, Q. Zhao de, M.X. Pan, W.H. Wang, Super plastic bulk metallic glasses at room temperature, Science, 315 (2007) 1385-1388.

[23] Q.S. Zhang, W. Zhang, G.Q. Xie, D.V. Louzguine-Luzgin, A. Inoue, Stable flowing of localized shear bands in soft bulk metallic glasses, Acta Mater., 58 (2010) 904-909.

[24] L.Y. Chen, Z.D. Fu, G.Q. Zhang, X.P. Hao, Q.K. Jiang, X.D. Wang, Q.P. Cao, H. Franz, Y.G. Liu, H.S. Xie, S.L. Zhang, B.Y. Wang, Y.W. Zeng, J.Z. Jiang, New class

of plastic bulk metallic glass, Phys. Rev. Lett., 100 (2008) 075501.

[25] J.J. Lewandowski, W.H. Wang, A.L. Greer, Intrinsic plasticity or brittleness of metallic glasses, Phil. Mag. Lett., 85 (2005) 77-87.

[26] X.J. Gu, A.G. McDermott, S.J. Poon, G.J. Shiflet, Critical Poisson's ratio for plasticity in Fe-Mo-C-B-Ln bulk amorphous steel, Appl. Phys. Lett., 88 (2006) 211905.

[27] W. Chen, K.C. Chan, S.F. Guo, P. Yu, Plasticity improvement of an Fe-based bulk metallic glass by geometric confinement, Mater. Lett., 65 (2011) 1172-1175.

[28] W. Chen, K.C. Chan, S.H. Chen, S.F. Guo, W.H. Li, G. Wang, Plasticity enhancement of a Zr-based bulk metallic glass by an electroplated Cu/Ni bilayered coating, Mater. Sci. Eng. A, 552 (2012) 199-203.

[29] L.W. Ren, Z. Wang, M.M. Meng, H. Tian, H.J. Yang, J.W. Qiao, Plasticity enhancement in bulk metallic glasses by electroless plating with Ni-P amorphous films, J. Non-Cryst. Solids, 430 (2015) 115-119.

[30] W.F. Wu, C.Y. Zhang, Y.W. Zhang, K.Y. Zeng, Y. Li, Stress gradient enhanced plasticity in a monolithic bulk metallic glass, Intermetallics, 16 (2008) 1190-1198.

[31] L.Y. Chen, Q. Ge, S. Qu, Q.K. Jiang, X.P. Nie, J.Z. Jiang, Achieving large macroscopic compressive plastic deformation and work-hardening-like behavior in a monolithic bulk metallic glass by tailoring stress distribution, Appl. Phys. Lett., 92 (2008) 211905.

[32] S.H. Chen, K.C. Chan, L. Xia, Effect of stress gradient on the deformation behavior of a bulk metallic glass under uniaxial tension, Mater. Sci. Eng. A, 574 (2013) 262-265.

[33] N. Li, Q. Chen, L. Liu, Size dependent plasticity of a Zr-based bulk metallic glass during room temperature compression, J. Alloys Compd., 493 (2010) 142-147.

[34] F.F. Wu, Z.F. Zhang, S.X. Mao, J. Eckert, Effect of sample size on ductility of metallic glass, Phil. Mag. Lett., 89 (2009) 178-184.

[35] L.W. Ren, M.M. Meng, Z. Wang, F.Q. Yang, H.J. Yang, T. Zhang, J.W. Qiao, Enhancement of plasticity in Zr-based bulk metallic glasses electroplated with copper coatings, Intermetallics, 57 (2015) 121-126.

[36] S.H. Chen, K.C. Chan, L. Xia, Deformation behavior of bulk metallic glass structural elements, Mater. Sci. Eng. A, 606 (2014) 196-204.

[37] J.X. Zhao, F.F. Wu, R.T. Qu, S.X. Li, Z.F. Zhang, Plastic deformability of metallic glass by artificial macroscopic notches, Acta Mater., 58 (2010) 5420-5432.

[38] W.H. Wang, R.J. Wang, G.J. Fan, J. Eckert, Formation and properties of Zr-(Ti, Nb)-Cu-Ni-Al bulk metallic glasses, Mater. Trans., 42 (2001) 587-591.

[39] G. Wang, K.C. Chan, L. Xia, P. Yu, J. Shen, W.H. Wang, Self-organized intermittent plastic flow in bulk metallic glasses, Acta Mater., 57 (2009) 6146-6155.

[40] B.A. Sun, H.B. Yu, W. Jiao, H.Y. Bai, D.Q. Zhao, W.H. Wang, Plasticity of Ductile Metallic Glasses: A Self-Organized Critical State, Phys. Rev. Lett., 105 (2010) 035501.

[41] T.G. Nieh, Y. Yang, J. Lu, C.T. Liu, Effect of surface modifications on shear banding and plasticity in metallic glasses: An overview, Prog. Nat. Sci., 22 (2012) 355-363.

[42] Z. Wang, J.W. Qiao, G. Wang, K.A. Dahmen, P.K. Liaw, Z.H. Wang, B.C. Wang, B.S. Xu, The mechanism of power-law scaling behavior by controlling shear bands in bulk metallic glass, Mater. Sci. Eng. A, 639 (2015) 663-670.

[43] X.L. Bian, G. Wang, K.C. Chan, J.L. Ren, Y.L. Gao, Q.J. Zhai, Shear avalanches in metallic glasses under nanoindentation: Deformation units and rate dependent strain burst cut-off, Appl. Phys. Lett., 103 (2013) 101907.

[44] T. Richeton, J. Weiss, F. Louchet, Breakdown of avalanche critical behaviour in polycrystalline plasticity, Nat. Mater., 4 (2005) 465-469.

[45] S.H. Chen, K.C. Chan, L. Xia, Deformation behavior of a Zr-based bulk metallic glass under a complex stress state, Intermetallics, 43 (2013) 38-44.

[46] C.J. Lee, Y.H. Lai, J.C. Huang, X.H. Du, L. Wang, T.G. Nieh, Strength variation and cast defect distribution in metallic glasses, Scripta Mater., 63 (2010) 105-108.

[47] S.H. Chen, K.C. Chan, G. Wang, F.F. Wu, L. Xia, J.L. Ren, J. Li, K.A. Dahmen, P.K. Liaw, Loading-rate-independent delay of catastrophic avalanches in a bulk metallic glass, Sci. Rep., 6 (2016) 21967.

[48] G. Kumar, A. Desai, J. Schroers, Bulk Metallic Glass: The Smaller the Better,

Adv. Mater., 23 (2011) 461-476.

[49] S.H. Chen, K.C. Chan, F.F. Wu, L. Xia, Pronounced energy absorption capacity of cellular bulk metallic glasses, Appl. Phys. Lett., 104 (2014) 111907.

[50] S.H. Chen, K.C. Chan, G. Wang, J. Yi, Saw-tooth-like bulk metallic glass structures with greatly enhanced energy-absorption performance, J. Alloys Compd., 661 (2016) 49-54.

Table I. The cut-off stress drops (σ_c) of three group specimens (A, B and D) at varying strain rates.

Strain rate (s^{-1})	Cut-off stress drop, σ_c (MPa)		
	Group A	Group B	Group D
5×10^{-3}	46.5	11.1	13.8
5×10^{-4}	48.3	39.8	14.9
5×10^{-5}	67.3	59.9	6.9

Table II. The dominant mechanisms of the plastic deformation behavior of BMGs on the change of strain rates under external disturbances, where *Multiple* denotes the multiplication of shear bands, and *Confinement* denotes the confinement of the propagation of shear bands.

External disturbances	From 5×10^{-3} to 5×10^{-4} s^{-1}	From 5×10^{-4} to 5×10^{-5} s^{-1}
No (A)	*Multiple*	*Multiple*
Geometric confinement (B)	*Confinement*	*Confinement*
Sample size (C)	*Multiple*	*Multiple*
Stress gradient (D)	*Confinement*	*Multiple + Confinement*

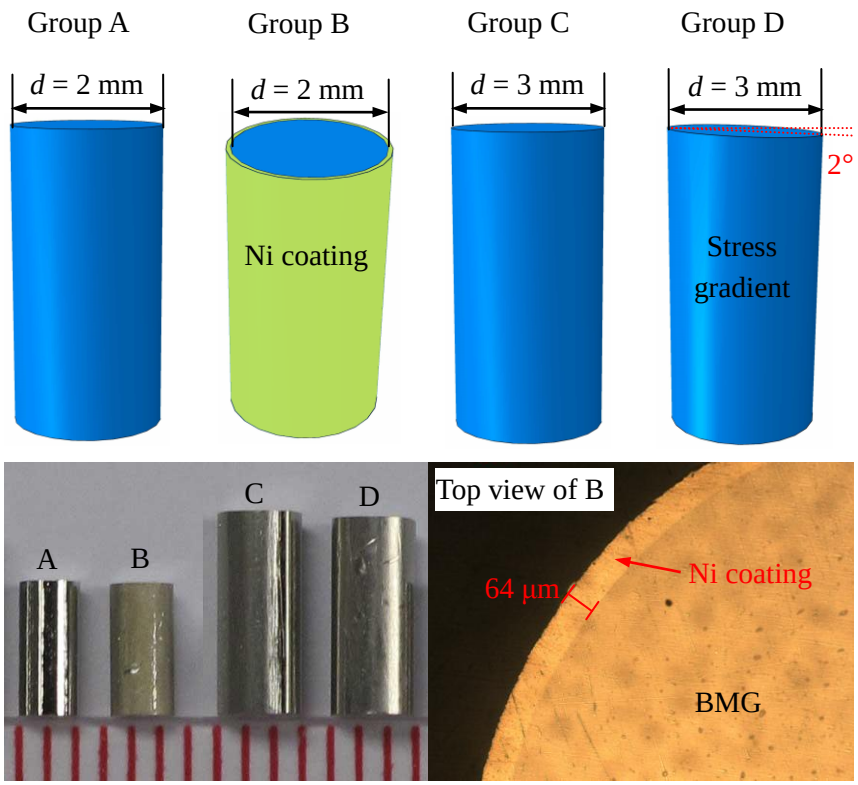

Fig. 1. Schematic diagrams of four groups of specimens, where the optical images show the four prepared specimens.

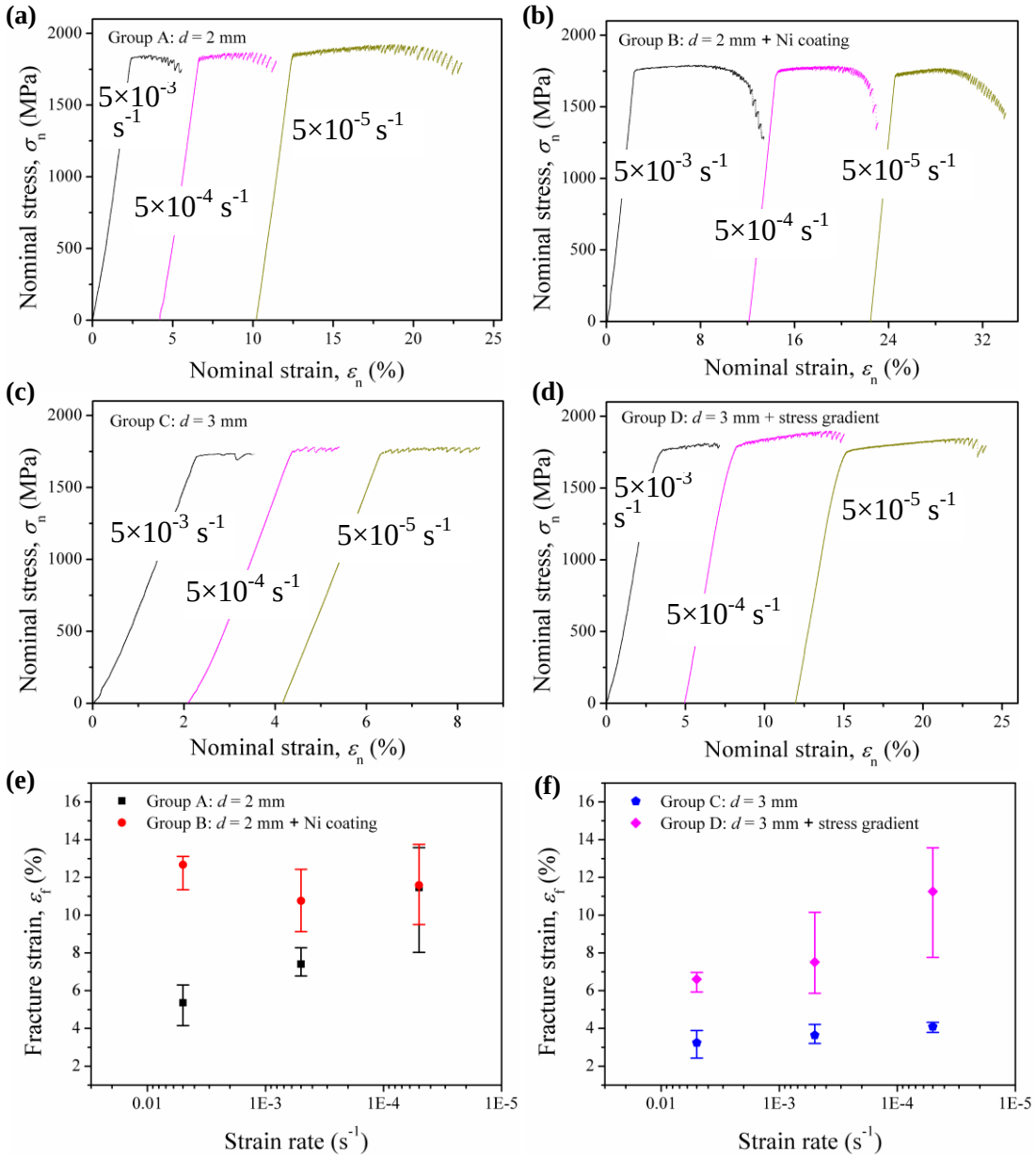

Fig. 2. (a-d) Typical nominal stress-strain curves of the specimens in Groups A-D, respectively, and (e,f) summarize the change of fracture strains at varying strain rates.

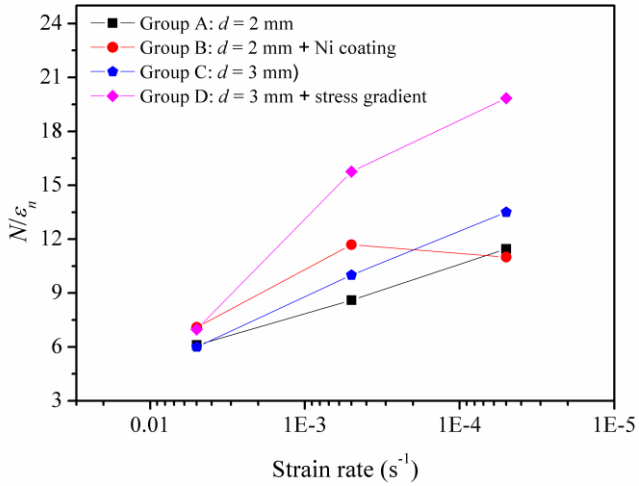

Fig. 3. The varying of the number of stress drops per 1% nominal strain (N/ε_n) of the four groups of specimens.

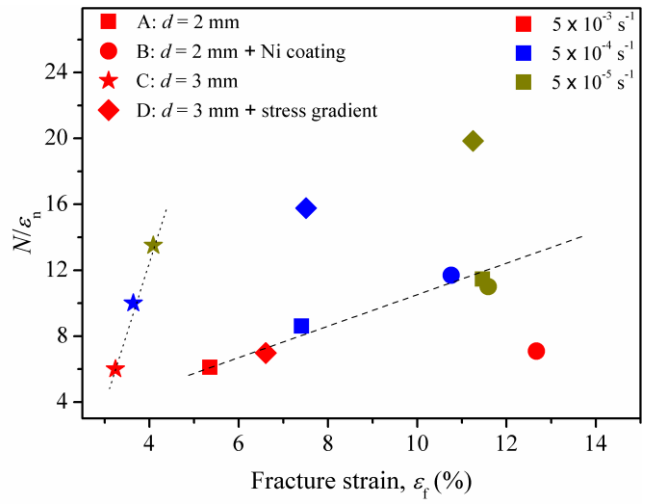

Fig. 4. Relationships between the number of stress drops per 1% nominal strain (N/ε_n) and the fracture strain (ε_n), where the symbol shows the group of the specimens and the symbol color indicates the corresponding strain rate.

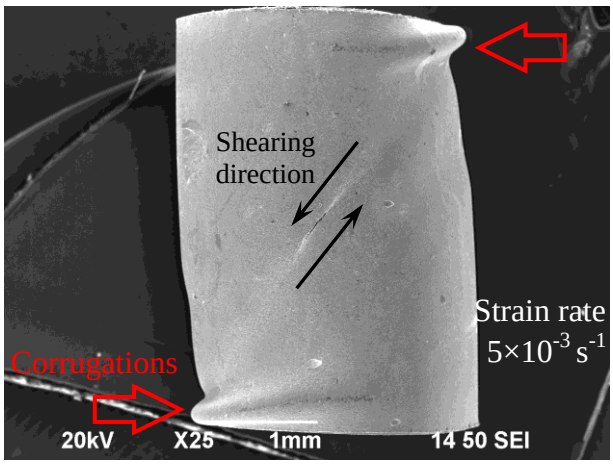

Fig. 5. SEM image of a deformed specimen in Group B, where the hollow arrows indicate the corrugated Ni-coatings and the solid arrows show the shearing direction before fracture.

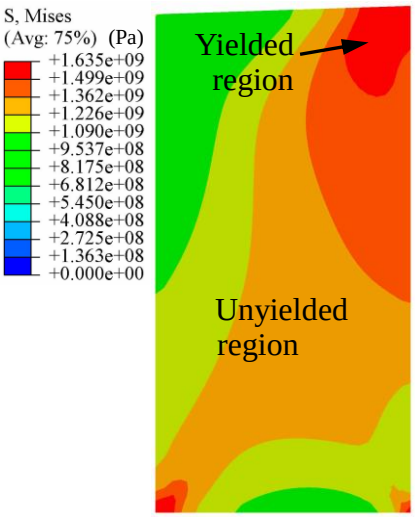

Fig. 6. FEM results showing the yielded regions in a Group D specimen at a nominal strain of about 2.25%.

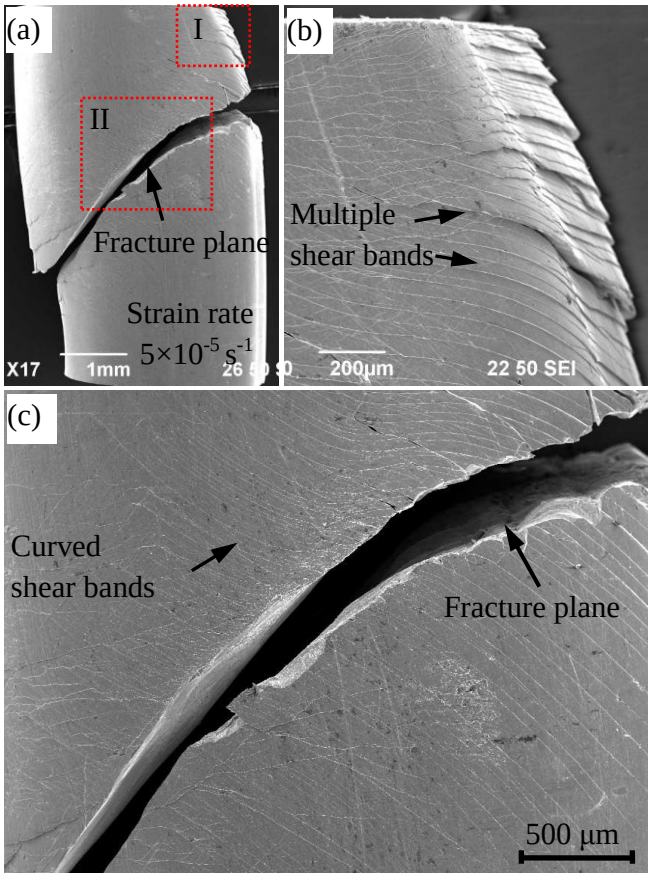

Fig. 7. (a) SEM image of a fractured specimen in Group D with a nominal strain of about 13.6 %, where the red rectangles I and II are magnified in (b) and (c) respectively.